Analytical and Bioanalytical Chemistry
https://doi.org/10.1007/s00216-018-1243-z

RESEARCH PAPER

# Selective non-enzymatic total bilirubin detection in serum using europium complexes with different β-diketone-derived ligands as luminescence probes

Wei Yang[1] · Jinfeng Xia[2] · Guohong Zhou[2] · Danyu Jiang[2] · Qiang Li[1] · Shiwei Wang[2] · Xiaohong Zheng[1] · Xi Li[1] · Yibo Shen[1] · Xin Li[1]

Received: 11 April 2018 / Revised: 11 June 2018 / Accepted: 4 July 2018
© Springer-Verlag GmbH Germany, part of Springer Nature 2018

## Abstract

Three europium(III) complexes, $Eu(ectfd)_3$ (Hectfd = 1-(9-ethyl-9H-carbazol-7-yl)-4,4,4-trifluorobutane-1,3-dione), $Eu(tta)_3$ (Htta = 4,4,4-trifluoro-1-(thiophen-2-yl)-butane-1,3-dione), and $Eu(dbt)_3$ (Hdbt = 2-(4',4',4'-trifluoro-1',3'-dioxobutyl)dibenzothiophene), were synthesized and employed to detect total bilirubin (BR) in blood-serum samples. UV-visible absorption and fluorescence (FL) spectroscopies were used to evaluate the selectivity of each europium (III) fluorescence probe to BR, which was shown to remarkably reduce the luminescence intensities of the europium(III) complexes at a wavelength of 612 nm. The luminescence intensity of each complex is linearly related to BR concentration. $Eu(tta)_3$ was shown to be the more-appropriate fluorescence probe for the sensitive and reliable detection of total BR in blood serum samples than either $Eu(ectfd)_3$ or $Eu(dbt)_3$. This observation can be ascribed to special σ-hole bonding between Htta and BR. In addition, the optimal pH test conditions for the detection of BR in human serum by the $Eu(tta)_3$ probe were determined. Sensitivity was shown to be dramatically affected by the pH of the medium. The experimental results reveal that pH 7.5 is optimal for this probe, which coincides with the pH of human serum. Furthermore, BR detection using the $Eu(tta)_3$ luminescence probe is simple, practical, and relatively free of interference from coexisting substances; it has a minimum detection limit (DL) of 68 nM and is a potential candidate for the routine assessment of total BR in serum samples.

**Keywords** Total bilirubin · Europium(III) complex · Biosensor · Fluorescence quenching · σ-hole

## Introduction

Bilirubin (BR) is the yellow metabolic breakdown product of normal blood and is of great biological and diagnostic importance [1]. It is a linear tetrapyrrole composed of two conjugated dipyrrole segments connected by labile methylene bridges [2]. The total BR concentration in blood is in the 6.0–17.1 μM range [3]. When the concentration exceeds this range, the additional BR in the body evokes a variety of diseases, including cirrhosis, acute or chronic hepatitis, cholestasis, primary level cancer, hemolytic anemia, and carcinoma of the pancreas [4]. Therefore, the ability to accurately measure BR concentrations is of great significance for the diagnosis of these diseases.

Many analytical methods have been developed for the determination of BR levels in serum samples [5]; these include modified diazo methods [6], BR-oxidase (BOx) and peroxidase-based oxidation methods, separation-based methods [7], electrochemical-biosensing [3], and fluorometric methods [8]. Among these methods, the currently used peroxidase-based method is complex, indirect, and requires multiple measurements. For the diazo method, accuracy is highly dependent on the testing pH. Although an enzyme-based biosensor can avoid interference caused by a number of biological substrates, it suffers from high cost and the low stability of enzymes, while in electrochemical biosensors the electrodes are easily contaminated by biological media.

✉ Qiang Li
qli@chem.ecnu.edu.cn

[1] Department of Chemistry, East China Normal University, Shanghai 200062, China

[2] Shanghai Institute of Ceramics, Chinese Academy of Sciences, Shanghai 200050, China

Published online: 25 July 2018

Hence, there is urgent need to explore and develop a novel nonenzymatic method for the rapid and reliable detection of total BR in blood-serum samples.

The fluorescent probes have excellent photophysical and living cell stability, and they are widely used in biology, such as cell imaging [9–11], cancer treatment [12], visually detecting β-galactosidase in vivo cells [13], and bisulfite in living zebrafish [14]. The fluorescence lifetime of the biomatrix is generally less than 3 ns. However, the fluorescence lifetime of the metal complexes-based fluorescence method is longer than this, which can effectively separate the detection signal from its strong background [9]. When the fluorescence method is bound to a specific protein, it can be further applied to the detection of epigenetics or DNA methylation [10]. The fluorescence imaging technology has many advantages in demonstrating the movement of living cell membranes [11] and detecting changes in specific components of cancer cells [12, 13]. A fluorometric method appears to be the most appropriate means of detecting BR; however, fluorescent BR probes have seldom been reported. The majority of reported methods use gold nanoparticles [15, 16] or lanthanide complexes [17]. Gold nanoparticles are suitable for use in biological testing as they are highly sensitive and have low toxicity [18]. However, gold nanoclusters are still unsatisfactory for use in fluorescence detection [19]. On the other hand, because of advantages such as high fluorescence quantum yields, strong luminescence, narrow luminescence bands, large Stokes' shifts, and long fluorescence lifetimes [20, 21], lanthanides have increasingly been used in recent years for biological detection [22–24]. β-Diketonates are ideal ligands for $Eu^{3+}$ [25, 26]; β-diketone-based europium complexes emit characteristic $Eu^{3+}$ fluorescence at 612 nm [27]. The use of these complexes as fluorescence probes also avoids potential background fluorescence emission interference from the biological surroundings.

In the present work, we developed a highly sensitive, inexpensive, and novel nonenzymatic spectrofluorimetric method. Three europium (III) complexes were synthesized; these complexes detect BR by the quenching of the luminescence intensities of their characteristic europium emissions at 612 nm. The function of the β-diketone-derived ligands is also discussed.

## Materials and methods

### Chemicals, reagents, and apparatus

BR and human serum albumin (HSA) were obtained from Sigma-Aldrich (USA). 9-Ethyl-9H-carbazole, dibenzothiophene, 4,4,4-trifluoro-1-(thiophen-2-yl)butane-1,3-dione, and $EuCl_3.6H_2O$ were obtained from J&K Chemicals. All chemicals and reagents in this study were of analytical grade and were used directly without further purification. Luminescence spectra were recorded on a FLS-980 spectrofluorometer (Edinburgh Instruments, UK) equipped with a quartz cuvette (1.0 cm × 1.0 cm) using 1 nm slit widths for excitation and emission. The UV–vis absorption spectra were recorded on an Agilent Cary UV-8000 spectrophotometer (Tianmei, China). The photoluminescence decays of the Eu(III) complexes were recorded on an FLS-980 spectrofluorometer (Edinburgh Instruments, UK) equipped with 356, 359, and 367 nm lasers.

### Synthesis of β-diketone derivate ligands

3-Acetyl-9-ethylcarbazole and 2-acetyldibenzothiophene were synthesized via modifications of methods reported in the literature [28]. $BiCl_3$ (10.25 g, 32.5 mmol) was added to a solution of dry 9-ethylcarbazole (3.90 g, 20.0 mmol) in anhydrous $CH_2Cl_2$ (50 mL). Acetyl chloride (3.925 g, 50.0 mmol) in anhydrous $CH_2Cl_2$ (5 mL) was added, followed by stirring for 2 h. A mixture of concentrated hydrochloric acid (25 mL) and water (15 mL) was then added. The organic phase was separated and the $CH_2Cl_2$ was removed by distillation. The residue was purified by silica-gel column chromatography with $CH_2Cl_2$ as the eluent. 2-Acetyldibenzothiophene was synthesized in an analogous fashion.

3-Acetyl-9-ethylcarbazole (2.37 g, 10.0 mmol), ethyl trifluoroacetate (2.84g, 20.0 mmol), and $CH_3ONa$ (0.81 g, 15.0 mmol) were stirred in anhydrous toluene (30 mL) for 12 h at 55 °C, after which the reaction mixture was poured into 15% HCl (25 mL). The organic phase was separated and the toluene was removed by distillation. The residue was purified by silica gel column chromatography to afford the pure product. Hdbt was synthesized in an analogous fashion. The synthesis of the ligands is shown in Scheme 1.

### Synthesis of $Eu(ectfd)_3$, $Eu(tta)_3$, and $Eu(dbt)_3$

$Eu(ectfd)_3$, $Eu(tta)_3$, and $Eu(dbt)_3$ were prepared by methods reported in the literature [29–32]. The three complexes (200 μmol) were then dissolved in ethanol (50 mL) for further use. All excitation, emission, and UV–vis spectra were measured at room temperature. Concentrations of $Eu^{3+}$, $Eu(ectfd)_3$, $Eu(tta)_3$, and $Eu(dbt)_3$ were maintained at 3 μM and excitation spectra were acquired in order to determine the response of the characteristic $Eu^{3+}$ emission at 612 nm. Emission spectra were then recorded at the strongest excitation wave length.

### Luminescence responses of $Eu(ectfd)_3$, $Eu(dbt)_3$, and $Eu(tta)_3$ to BR

Aliquots (2 mL) containing Tris-HAc buffer (pH = 7.5), $Eu(ectfd)_3$, $Eu(tta)_3$, or $Eu(dbt)_3$ (3 μM) as the luminescence probe, and a 100 μL aliquot of a serum sample containing BR

**Scheme 1** A synthetic procedure for ligands (Hdbt, Hectfd )

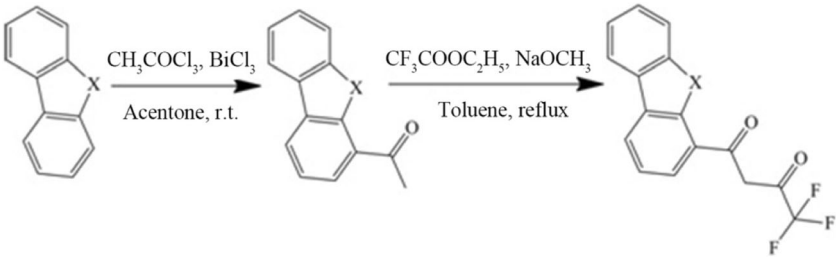


(1–70 μM) were equilibrated at room temperature (RT). Luminescence spectra were recorded at excitation wavelengths of 356, 359, and 367 nm for $Eu(ectfd)_3$, $Eu(tta)_3$, and $Eu(dbt)_3$, respectively. Luminescence responses towards different concentrations of BR were determined in triplicate to provide average values. The selectivity of each assay was evaluated by measuring the luminescence intensity of $Eu(ectfd)_3$, $Eu(tta)_3$, or $Eu(dbt)_3$ in the presence of a variety of other relevant substances that are present in blood serum, such as albumin, galactose, glucose, fructose, urea, uric acid, glutathione, and cholesterol (100 μM each). A plot of relative luminescence intensity ($F_0/F$) as a function of interfering substance was also generated. The effect of different values of solution pH on the response of $Eu(tta)_3$ towards 10 μM BR was studied using different Tris-HAc buffers.

## Results and discussion

### Luminescence properties of Eu complexes with different β-diketone-derived ligands and their luminescence responses to BR

The excitation and emission spectra of $Eu^{3+}$, $Eu(ectfd)_3$, $Eu(tta)_3$, and $Eu(dbt)_3$ are displayed in Fig. 1; the latter were obtained by excitation at 272, 359, 356, and 367 nm, respectively. The emission maxima of $Eu^{3+}$ and the three complexes are all centered at 612 nm, which is characteristic of $Eu^{3+}$ and is the result of the $^5D_0$–$^7F_2$ transition of $Eu^{3+}$. As can be seen in Fig. 1, the $Eu^{3+}$ luminescence intensity is effectively enhanced by Hectfd, Htta, and Hdbt. At the same time, the excitation wavelength is shifted from 272 nm ($Eu^{3+}$) to 359, 356, and 367 nm for $Eu(ectfd)_3$, $Eu(tta)_3$, and $Eu(dbt)_3$, respectively. The phenomenon described above is the result of the antenna effect, which demonstrates that Hectfd, Htta, and Hdbt are ideal ligands for $Eu^{3+}$. After Hectfd, Htta, and Hdbt become coordinated to $Eu^{3+}$, emission peaks corresponding to Htta and Hdbt are absent in the emission spectra of $Eu(tta)_3$ and $Eu(dbt)_3$, while $Eu(ectfd)_3$ exhibits a weak emission peak for Hectfd at 495 nm.

Owing to these good luminescence properties, the luminescence responses of the $Eu(L)_3$ ($L$ = ectfd, tta, or dbt) clusters in the presence of different concentrations of BR (nine separate concentration in the 1–70 μM range) were investigated. Excitation of $Eu(L)_3$ at 359, 356, or 367, with luminescence monitoring in the 420–750 nm range, revealed that the intensity of the $Eu(L)_3$ luminescence emission at 612 nm gradually decreases with increasing BR concentration, as shown in Fig. 2a–c; at a BR concentration of 70 μM, the luminescence intensity of $Eu(tta)_3$ is almost completely quenched (Fig. 2b). In order to investigate the selectivity of this method for the detection of BR, interference studies were performed through the addition of foreign substances commonly present in the blood serum, including fructose, glucose, galactose, urea, uric acid, cholesterol, and human serum albumin (HSA). The relative luminescence of $Eu(ectfd)_3$, $Eu(tta)_3$, and $Eu(dbt)_3$ are represented by $F_0/F$, where $F$ and $F_0$ are the luminescence intensities of $Eu(L)_3$ with and without BR, respectively, and the relationships between $F_0/F$ and the different serum compounds are presented in Fig. 2d, which reveals that only BR facilitates a significant decrease in luminescence intensity, while the other compounds do not induce any obvious variations in luminescence intensity. $Eu(tta)_3$ exhibits excellent sensitivity and specificity for BR. At a BR concentration of 30 μM, the relative fluorescence, $F_0/F$, of $Eu(tta)_3$ is 23.1; the other substances (100 μM) interfere little with the response of $Eu(tta)_3$ to BR. The BR-specific selectivity of $Eu(tta)_3$ is far greater than that of other fluorescence probes [15, 17, 33]. In comparison, the relative luminescence of $Eu(ectfd)_3$ and $Eu(dbt)_3$ are 3.2 and 5.6, respectively, which are considerably lower than that of $Eu(tta)_3$.

Compared with the other methods for the detection of BR listed in Table 1, the $Eu(tta)_3$ luminescence probe has distinct advantages. It has a lower detection limit than fiber-optic sensors or chemiluminescence, while, at the same time, the linear-response range of $Eu(tta)_3$ to BR is larger than that of the fluorimetric-enzymatic method or BR-oxidase enzymatic analysis. The detection method is easy to operate and does not require the separation of impurities in the serum. Owing to the unique luminescence properties of lanthanide complexes, this method is not subject to biological background luminescence interference. A new type of luminescence probe for the determination of BR is introduced in this paper; $Eu(tta)_3$ integrates excellent linearity with sensitivity and is an effective fluorescence probe for the following work.

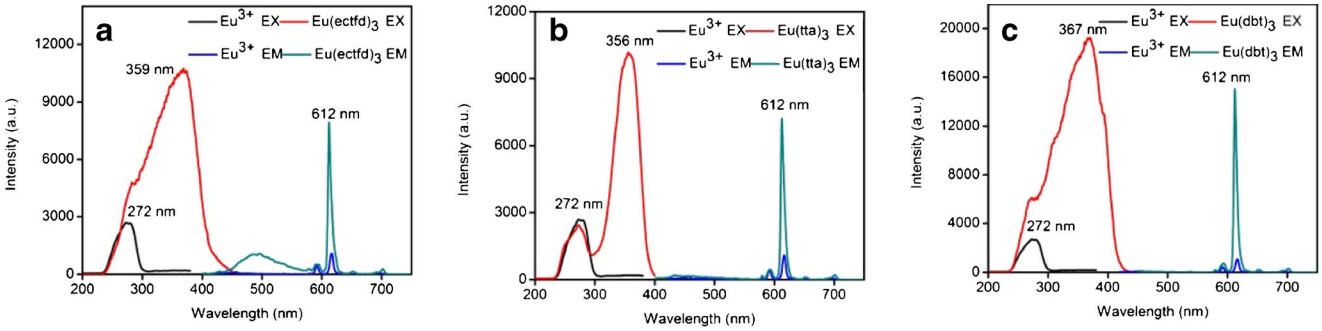


**Fig. 1** Excitation spectra and emission spectra of $Eu^{3+}$, $Eu(ectfd)_3$ **(a)**, $Eu^{3+}$, $Eu(tta)_3$ **(b),** and $Eu^{3+}$, $Eu(dbt)_3$ **(c)**.

## Interactions of BR with $Eu(ectfd)_3$, $Eu(dbt)_3$, and $Eu(tta)_3$

Based on the different luminescence responses of $Eu(ectfd)_3$, $Eu(dbt)_3$, and $Eu(tta)_3$, the interaction mechanism of BR with Eu complexes was studied. There are two possible interactions: between BR and $Eu^{3+}$, or between BR and the β-diketone-derived ligand. Figure 3 displays the UV–vis absorption spectra of $Eu^{3+}$, *L*, BR, $Eu(L)_3$, *L*/BR, $Eu^{3+}$/BR, and $Eu(L)_3$/BR. The ligands exhibit broad bands in the 300–400 nm range that are attributable to singlet–singlet $\pi \rightarrow \pi^*$ enol absorptions [41], and are characteristic of the enol forms of β-diketones. The absorption spectra of the three complexes are blue shifted to different degrees in comparison with the spectra of the corresponding free ligands. The absorption spectral profiles of the various complexes are similar to those of the corresponding free ligand, indicating that the β-diketonate ligands contribute to the absorption of the complexes. On the other hand, according to previous research, a superposition of the two electronic transitions generated in the AB and CD chromophores, with one centered around 480 nm and the other around 430 nm [42], as shown in Scheme 2, results in a dominant BR absorption band at around 450 nm. Comparisons of the absorption spectrum of BR with those of *L*/BR, $Eu^{3+}$/BR, and $Eu^{3+}$/*L*-BR are presented in Fig. 3. It is interesting to find that the addition of *L*, $Eu^{3+}$, or $Eu^{3+}$/*L* to BR solution does not alter the BR absorption peak; at the same time, no other peaks appear. As reported in the literature [43, 44], when BR is coordinated to $Eu^{3+}$, its absorption maximum shifts from 450 to 387 nm. The data in Fig. 3 reveal that BR

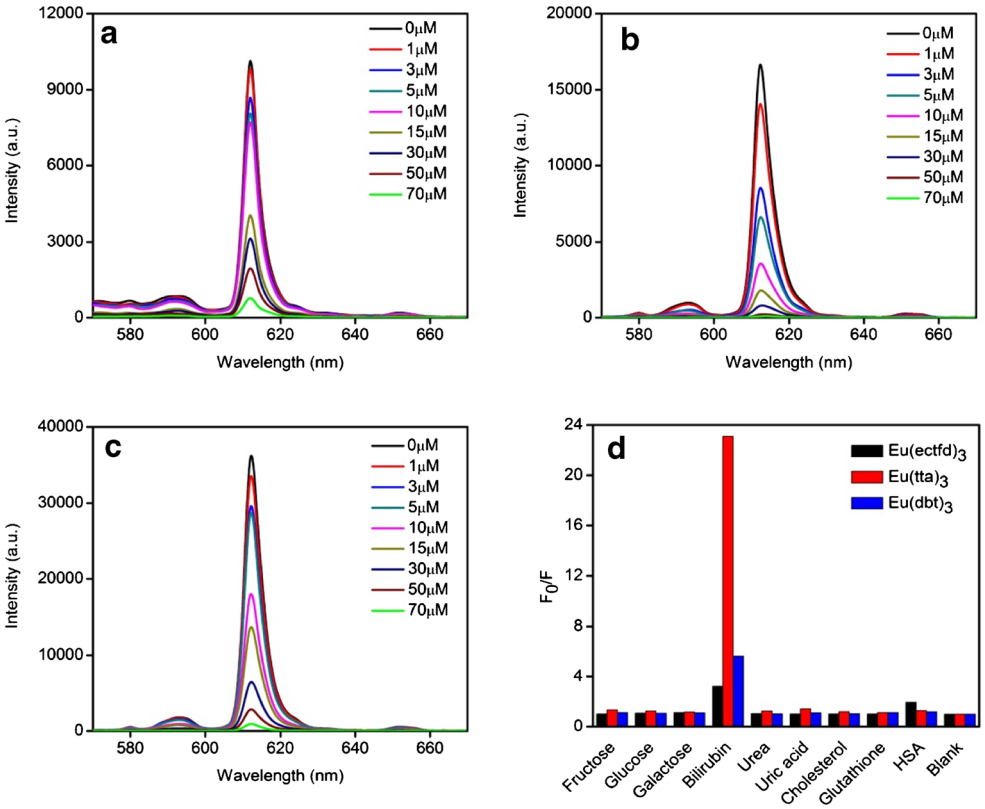


**Fig. 2** The emission spectra of the complexes $Eu(ectfd)_3$ **(a)**; $Eu(tta)_3$ **(b)**; and $Eu(dbt)_3$ **(c)** in the presence of different concentrations of BR (0–70 mM). Relative fluorescence ($F_0/F$) of $Eu(ectfd)_3$, $Eu(tta)_3$, and $Eu(dbt)_3$ in presence of bilirubin (30 mM) and various compounds 100 mM each **(d)**

**Table 1** Comparison of the methods for the determination of BR

| Method | Linear range | Detection limit | References |
|---|---|---|---|
| HPLC | 0 to 342 μmol $L^{-1}$ | 0.0005 nM | [34] |
| Fluorimetric-enzymatic method | Up to 12 μmol $L^{-1}$[a] | 2.6 nM[b] | [35] |
| Capillary micellar electrokinetic | 5.3 to 510 μmol $L^{-1}$ | — | [36] |
| Fiber optic sensor | 0.1 to 300 μmol $L^{-1}$ | 100 nM | [37] |
| BR oxidase enzymatic analysis | 0.34 to 2.9 μmol $L^{-1}$[c] | — | [38] |
| Chemiluminescence | 8.6 to 210 μmol $L^{-1}$[d] | 3100 nM[e] | [39] |
| Chemiluminescence | 0.1 to 100 μmol $L^{-1}$[f] | 13000 nM[g] | [40] |
| Fluorescent probe $Eu(tta)_3$ | 0 to 50 μmol $L^{-1}$ | 68 nM | — |

The following data were taken from the original literature: [a] up to 7 mg $L^{-1}$; [b] 1.5 μg $L^{-1}$; [c] 0.2–1.7 mg $L^{-1}$; [d] 5–120 mg $L^{-1}$; [e] 1.8 mg $L^{-1}$; [f] 0.0585–58.47 μg $mL^{-1}$; [g] 7.8826 μg $mL^{-1}$

does not coordinate to $Eu^{3+}$ and that no new complexes are generated. This conclusion is different from the reported quenching mechanism, which states that ligands first form binary complexes with $Eu^{3+}$, after which BR coordinates to the binary complexes to form ternary complexes [17, 18]. It is clear that the luminescence quenching of the above $Eu^{3+}$ complexes is accompanied by interactions between BR and the ligands.

In order to determine the reason for the different responses of $Eu(ectfd)_3$, $Eu(dbt)_3$, and $Eu(tta)_3$ to BR, the relationship between the luminescence emission spectra of the β-diketone ligands and the absorption spectrum of BR is discussed. The Hectfd, Htta, and Hdbt ligands were excited at 420, 370, and 383 nm, respectively. Figure 4 shows that Hectfd, Htta, and Hdbt are luminescent, with wavelength maxima of 482, 456, and 473 nm, respectively. The gray regions in Fig. 4 highlight the overlapping areas of the ligand emission spectra and the BR absorption spectrum. The emission profile of Htta overlaps the most with the absorption profile of BR (Fig. 4b), while that of Hectfd overlaps the least (Fig. 4a). According to Föster's non-radioactive energy-transfer theory [45], the greater the overlapping areas, the more the ligands deliver energy to BR; consequently, energy transfer from Htta to BR occurs more efficiently than from either Hectfd or Hdbt.

Owing to the antenna effect, when $L$ is coordinated to $Eu^{3+}$ it transfers its absorbed energy to the $Eu^{3+}$, and $Eu^{3+}$ emits at its characteristic wavelength. When BR is added to a solution of $Eu(L)_3$, L transfers part of its absorbed energy to BR. Consequently, less energy is transferred to $Eu^{3+}$ than in the absence of BR; clearly, the luminescence intensity of $Eu^{3+}$ decreases as a result. This quenching process is described by the following equilibrium:

$$[C] + n[Q] \rightarrow [C{-\!-}nQ] \quad \left(C = Eu(ectfd)_3, Eu(tta)_3, \text{or } Eu(dbt)_3\right),$$

where the coordinated ligands pass energy to $n$ equivalents of nearby BR, and [Q] is the concentration of BR. The fluorescence of $Eu(ectfd)_3$, $Eu(tta)_3$, and $Eu(dbt)_3$ are quenched as a result of the above process. Regression curves were plotted using the following equations [46, 47]:

$$K_A = \frac{[C{-\!-}nQ]}{[C][Q]^n} = \frac{[C_0]-[C]}{[C][Q]^n} \quad (1)$$

$$\frac{[C]}{[C_0]} = \frac{F}{F_0} \quad (2)$$

$$K_A[Q]^n = \frac{F_0 - F}{F} \quad (3)$$

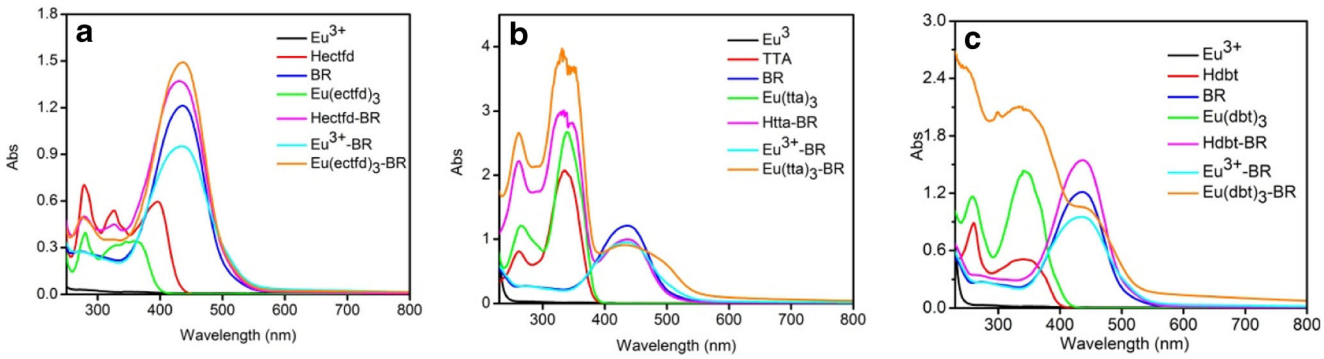


**Fig. 3** Absorption spectra of $Eu^{3+}$, Hectfd, BR, $Eu(ectfd)_3$ Hectfd-BR, $Eu^{3+}$-BR, and $Eu(ectfd)_3$-BR **(a )**, $Eu^{3+}$, Htta, BR, $Eu(tta)_3$ Htta-BR, $Eu^{3+}$-BR, and $Eu(tta)_3$-BR **(b),** $Eu^{3+}$, Hdbt, BR, $Eu(dbt)_3$ Hdbt-BR, $Eu^{3+}$-BR, and $Eu(dbt)_3$ **(c)**. The concentrations of the test solutions: $Eu^{3+}$, $3.0 \times 10^{-6}$ mol $L^{-1}$; L, $3.0 \times 10^{-6}$ mol $L^{-1}$; BR, $1.0 \times 10^{-5}$mol $L^{-1}$, $Eu(L)_3$, $3.0 \times 10^{-6}$ mol $L^{-1}$, respectively; buffer, pH =7.40. The results were obtained after standing for 15 min at room temperature and measured using a UV-8000 recording spectrophotometer

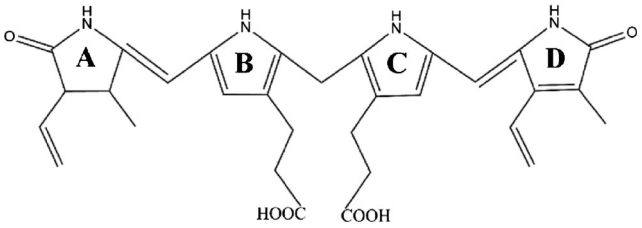


**Scheme 2** The chemical structure of BR

$$\lg\frac{F_0-F}{F} = \lg K_A + n\lg[Q] \quad (4)$$

where $C$ and $C_0$ are the complexes with and without BR; $F$ and $F_0$ are the luminescence intensities of Eu($L$)$_3$ with and without BR, respectively.

Fluorescence response curves for Eu($L$)$_3$ against BR were generated using Eq. 4, lg(($F_0$-$F$)/$F$) = lg $K_A$ + $n$ lg[BR]. The logarithm of the luminescence intensity, lg(($F_0$-$F$)/$F$), is directly proportional to the logarithm of the BR concentration, lg[BR], over the 1–70 μM concentration range, as is seen in Fig. 5. The limit of detection ($C_{LOD}$) is defined by IUPAC to be the lowest concentration or amount of material, target, or analyte that is consistently able to be detected [48]; $C_{LOD}$ = 3 $Sb/m$ (where $Sb$ is the standard deviation of the blank signal and $m$ is the slope of the calibration graph) [17]. In this experiment, the limits of detection of Eu(ectfd)$_3$, Eu(tta)$_3$, and Eu(dbt)$_3$ were determined to be 204, 226, and 68 nM, respectively. Compared with Eu(ectfd)$_3$ and Eu(dbt)$_3$, Eu(tta)$_3$ exhibits better linearity ($R^2$ = 0.98) and better sensitivity, with a detection limit of 68 nM at a signal to noise ratio of 3.

Energy transfer efficiency is seriously affected by the number of adjacent BR molecules. The number of adjacent BR molecules ($n$) around Eu(ectfd)$_3$, Eu(dbt)$_3$, and Eu(tta)$_3$ are given by the slopes of their respective lines of best fit to Eq. 4, namely 0.96, 1.56, and 1.43, respectively. The values of n for Eu(tta)$_3$ and Eu(dbt)$_3$ are clearly greater than 1, while that of Eu(ectfd)$_3$ is close to 1. The molecular structures of tta and dbt both contain thiophene groups. Thiazole, a similar sulfur-containing heterocycle, is important in molecular biology and in pharmacology; it has the ability to form inter- and/or intramolecular noncovalent interactions [49-–51], including σ-holes. The high values of n for Eu(tta)$_3$ and Eu(dbt)$_3$ are

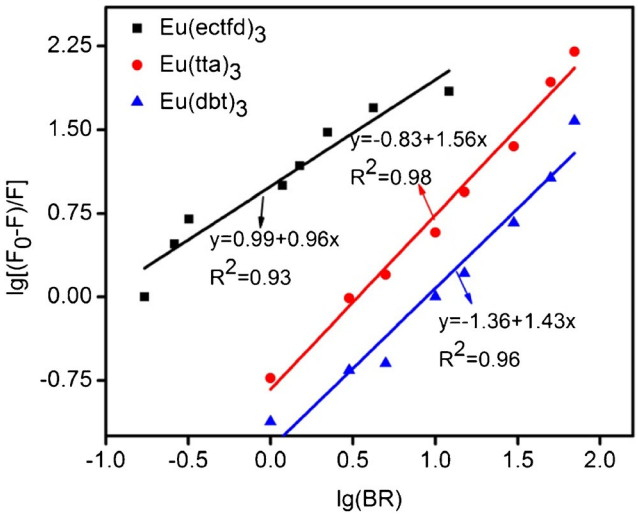


**Fig. 5** Plot of lg[($F_0$-$F$)/$F$] as a function of lg[BR]

mainly due to σ-hole bonding between the S atom in the thiophene of tta or dbt and the carbonyl oxygen atom of BR. σ-Holes [49] are widespread in biological systems [50–52]; in particular, they greatly influence the spatial structures of proteins. Furthermore, the trifluoromethyl groups in Htta and Hdbt, which are strongly electron-withdrawing, increase the positive charges on their thiophene sulfur atoms, thereby enhancing the σ-holes. As shown in Scheme 3, the O=C at the head of BR has sufficient electrons to act as a donor. The different molecular structures of the three ligands lead to different interactions with BR, as shown in Scheme 3; the unique molecular structures of Htta and Hdbt lead to intermolecular noncovalent interactions with BR (Scheme 3). The interactions between Eu(dbt)$_3$ and BR, and Eu(tta)$_3$ and BR, are similar, with the exception that the benzene rings of Hdbt weakly affect the positive charge of the S and provide steric hindrance that prevents BR from approaching. This also explains why the number of BR molecules adjacent to Eu(dbt)$_3$ is similar to that of Eu(tta)$_3$, but slightly less than that of Eu(tta)$_3$. However, there is almost no σ-hole bonding between N and O=C when compared with that involving S and O=C [53], which also explains why the n value of Eu(ectfd)$_3$ is far less than that of either Eu(tta)$_3$ or Eu(dbt)$_3$. On the one hand,

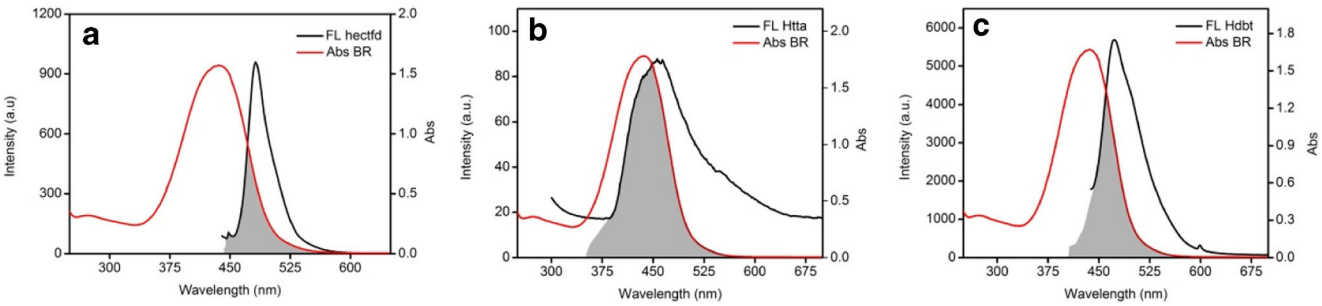


**Fig. 4** A The overlap of the fluorescence emission spectra Hectfd **(a)**, Htta **(b),** and Hdbt **(c)** with absorption spectra of BR

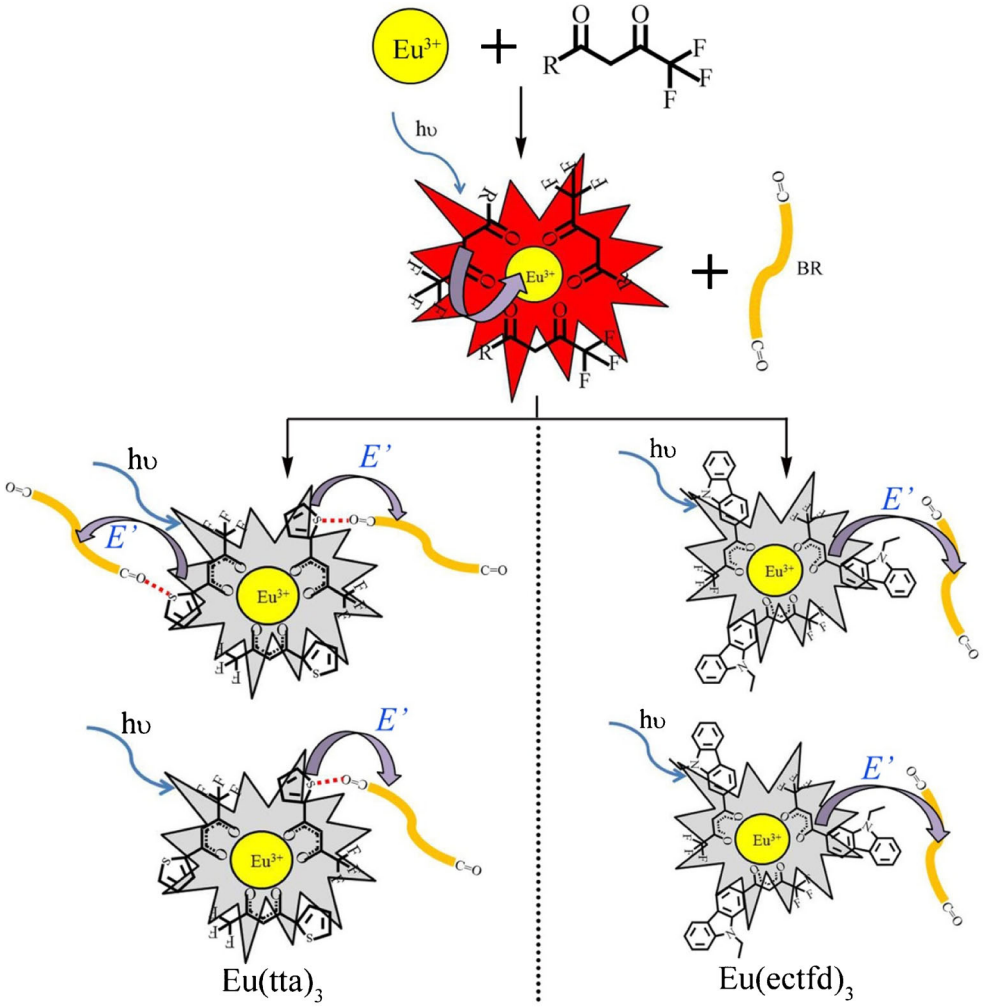


**Scheme 3** Energy transfer mechanism of BR quenching $Eu(L)_3$ fluorescence

σ-hole bonding enriches BR molecules near the $Eu^{3+}$ complex; on the other hand, it shortens the distance between the BR molecule and the β-diketone ligands. Ultimately, energy transfer from the β-diketone ligands to BR will be accelerated. Furthermore, σ-hole bonding also enhances the selectivity of the luminescence probe.

During luminescence processes, energy transfer changes are usually accompanied with variations in lifetime. The luminescence lifetimes of $Eu(ectfd)_3$, $Eu(tta)_3$, $Eu(dbt)_3$ and the complexes formed by mixing them with 50 μM BR were also measured; the decay constants from this study are presented in Fig. 6. Upon mixing with BR, the decay time of $Eu(tta)_3$ decreased from 316 to 200 μs, that of $Eu(dbt)_3$ decreased from 284 to 274 μs, while the decay time of $Eu(ectfd)_3$ was almost unchanged. These results are consistent with our previous experimental conclusions, since the number of BR molecules around $Eu(tta)_3$ is higher than that of $Eu(ectfd)_3$ and $Eu(dbt)_3$, and the energy of Htta

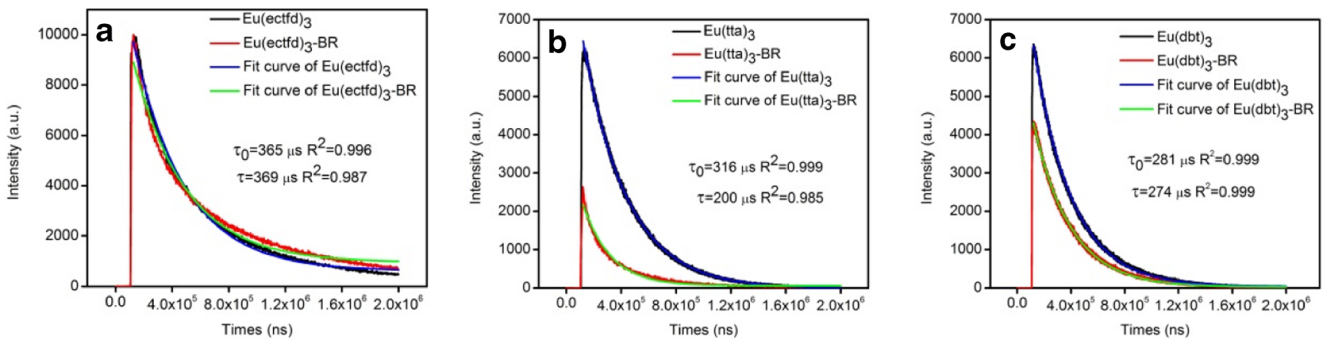


**Fig. 6** Fluorescence lifetime of $Eu(ectfd)_3$ **(a)**, fluorescence lifetime of $Eu(tta)_3$ **(b)**, and fluorescence lifetime of $Eu(dbt)_3$

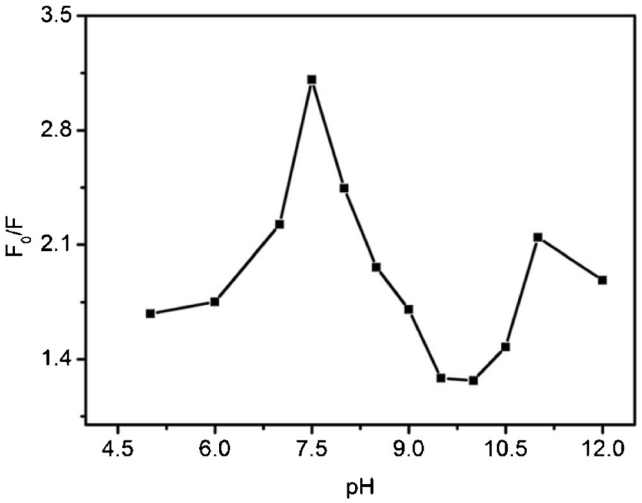


**Fig. 7** The influence of pH on the reduced luminescence intensity of $Eu(tta)_3$–BR system. A 3.0 mL buffer solution contains $Eu(tta)_3$ $3.0 \times 10^{-6}$ mol $L^{-1}$; BR $5.0 \times 10^{-5}$ mol $L^{-1}$

is best matched to that of BR among the complexes in this study. The test results also confirm that BR interferes with the process by which ligands transfer energy to $Eu^{3+}$ [54].

## Effect of pH on $Eu(tta)_3$ and detection of BR in human serum

Usually pH is an important factor for detection processes. In the present research, different pH values were achieved by adjusting the concentration of the Tris–HCl buffer solution. Figure 7 reveals that the relative luminescence intensity ($F_0/F$) of the system containing $Eu(tta)_3$ (3 μM) and BR (50 μM) is dramatically affected by the pH of the medium. The experimental results reveal a maximum $F_0/F$ value at pH 7.5, which conincides with that of human serum. Therefore, $Eu(tta)_3$ is a very convenient probe for determining BR levels in human serum.

The developed method was also examined for its ability to determine the BR content of human serum samples, which was conducted following previously reported protocols [5, 8, 9, 42]. Fresh human blood samples were collected from healthy volunteers. All experiments were performed in accordance with the Guidelines "Declaration of Helsinki (2002 edition)" and "Measures for Ethical Review of Biomedical Research involving People", and experiment approved by "The Academic Ethics Committee of East China Normal university". These samples were centrifuged at 4000 rpm for 20 min to isolate the serum. The serum sample (2.5 mL) was mixed with acetonitrile (2.5 mL) to precipitate proteins, after which the mixture was centrifuged at 6000 rpm for 60 min. The supernatant was then collected and evaporated under vacuum to remove the remaining acetonitrile. The solution obtained in this manner was stored at 4 °C for further use [8, 43]. Prepared serum samples were divided into four batches. Standard solutions containing 1, 4, 6, and 25 μM of BR were added to each of the four serum samples. The developed method was then used to determine the concentrations of BR added to the serum samples. The detection system contained 3 μM of $Eu(tta)_3$ to which 2 mL of each serum sample containing different concentrations of BR were added. The results of these experiments are listed in Table 2. The proposed method exhibits good recoveries and acceptable RSD values, as shown in Table 2, which verifies the accuracy and reliability of this method for the determination of BR in human serum. The same human serum sample was tested by a Chinese hospital and $Eu(tta)_3$, and the results were 13.4 μM and 13.8 μM, respectively. The recovery was calculated as 103%, which is in an acceptance range. These results suggest that the $Eu(tta)_3$ sensing probe has great potential for the quantitative determination of BR in real samples.

**Table 2** Determination of BR in serum samples

| Sample | Spiked amount (μM)) | Detected amount (μM)) ± | RSD[a] (%) | Recovery (%) |
|---|---|---|---|---|
| A | 1 | 1.16 | 2.25 | 116 |
| B | 4 | 3.95 | 4.06 | 98.8 |
| C | 6 | 6.08 | 3.36 | 101.3 |
| D | 25 | 24.75 | 4.73 | 99 |

[a] Please denote in footnote.

## Conclusions

New spectrofluorimetric probes based on $Eu^{3+}$ complexes with different β-diketone-derived ligands were developed for the determination of BR. Among three similar $Eu^{3+}$ complexes,$Eu(tta)_3$ exhibited the best sensitivity and selectivity, which is attributed to two factors: (1) the Htta emission profile overlaps the best with the BR absorption profile, and (2) the molecular structure of tta can form strong σ-hole bonds to BR. The optimal pH for detection (7.5) and the detection results from human serum samples confirm the accuracy and reliability of the $Eu(tta)_3$ probe for the determination of BR; $Eu(tta)_3$ has great potential for the quantitative determination of BR in real samples.

## Compliance with ethical standards

**Conflicts of interest** There are no conflicts to declare.

## References

1. Pendse A, Jasani B, Nanavati R, Kabra N. Comparison of transcutaneous bilirubin measurement with total serum bilirubin levels in preterm neonates receiving phototherapy. Indian Pediatr. 2017;54(8):641–3.

2. I. Taurino, V. Van Hoof, A. Magrez, L. Forro, G. De Micheli, S. Carrara (2014) Efficient voltammetric discrimination of free bilirubin from uric acid and ascorbic acid by a CVD nanographite-based microelectrode. Talanta 130 (5):423–426
3. Balamurugan T, Berchmans S. Nonenzymatic detection of bilirubin based on a graphene–polystyrene sulfonate composite. RSC Adv. 2015;5(62):50470–7.
4. Wang J, Wu X, Li Y, Han X, Hu H, Wang F, et al. Serum bilirubin concentrations and incident coronary heart disease risk among patients with type 2 diabetes: the Dongfeng-Tongji cohort. Acta Diabetol. 2017;54:257–2564.
5. Martelanc M, Ziberna L, Passamonti S, Franko M. Direct determination of free bilirubin in serum at sub-nanomolar levels. Anal Chim Acta. 2014;809:174–82.
6. Kannan P, Chen H, Lee VT, Kim DH. Highly sensitive amperometric detection of bilirubin using enzyme and gold nanoparticles on sol-gel film modified electrode. Talanta. 2011;86(86):400–7.
7. M. Martelanc, L. Ziberna, S. Passamonti, M. Franko (2016) Application of high-performance liquid chromatography combined with ultra-sensitive thermal lens spectrometric detection for simultaneous biliverdin and bilirubin assessment at trace levels in human serum. Talanta 154:92–98
8. Llorent-Martínez EJ, Durán GM, Ríos Á, Ruiz-Medina A. Graphene quantum dots-terbium ions as novel sensitive and selective time-resolved luminescent probes. Anal Bioanal Chem. 2017;410:1–418.
9. Vellaisamy K, Li G, Ko C-N, Zhong H-J, Fatima S, Kwan H-Y, et al. Cell imaging of dopamine receptor using agonist labeling iridium(III) complex. Chem Sci. 2017;9(5):1119–25.
10. Hori Y, Otomura N, Nishida A, Nishiura M, Umeno M, Suetake I, et al. Synthetic-molecule/protein hybrid probe with fluorogenic switch for live-cell imaging of DNA methylation. J Am Chem Soc. 2018;140:1686–90.
11. Wang H, Feng Z, Sj DS, Rodal AA, Xu B. Active probes for imaging membrane dynamics of live cells with high spatial and temporal resolution over extended time scales and areas. J Am Chem Soc. 2018;140:3505–409.
12. Liu L-J, Wang W, Huang S-Y, Hong Y, Li G, Lin S, et al. Inhibition of the Ras/Raf interaction and repression of renal cancer xenografts in vivo by an enantiomeric iridium(III) metal-based compound. Chem Sci. 2017;8(7):4756–63.
13. Wang W, Vellaisamy K, Li G, Wu C, Ko C-N, Leung C-H, et al. Development of a long-lived luminescence probe for visualizing β-galactosidase in ovarian carcinoma cells. Anal Chem. 2017;89(21): 11679–84.
14. Liu JB, Yang C, Ko C-N, Vellaisamy K, Yang B, Lee M-Y, et al. A long lifetime iridium(III) complex as a sensitive luminescent probe for bisulfite detection in living zebrafish. Sensors Actuators B. 2016;243:971–6.
15. Santhosh M, Chinnadayyala SR, Kakoti A, Goswami P. Selective and sensitive detection of free bilirubin in blood serum using human serum albumin stabilized gold nanoclusters as fluorometric and colorimetric probe. Biosens Bioelectron. 2014;59(5):370–6.
16. M. Santhosh, S.R. Chinnadayyala, N.K. Singh, P. Goswami (2016) Human serum albumin-stabilized gold nanoclusters act as an electron transfer bridge supporting specific electrocatalysis of bilirubin useful for biosensing applications. Bioelectrochemistry 111:7–14
17. Kamruzzaman M, Alam A-M, Lee SH, Kim YH, Kim G-M, Hyub S, et al. Spectrofluorimetric quantification of bilirubin using yttrium–norfloxacin complex as a fluorescence probe in serum samples. J Lumin. 2012;132(11):3053–7.
18. Liang J, Xiong H, Wang W, Wen W, Zhang X, Wang S. Luminescent-off/on sensing mechanism of antibiotic-capped gold nanoclusters to phosphate-containing metabolites and its antibacterial characteristics. Sensors Actuators B. 2018;255:2170–8.
19. Sasidharan A, Monteiro-Riviere NA. Biomedical applications of gold nanomaterials: opportunities and challenges. Wiley Interdiscip Rev: Nanomed Nanobiotechnol. 2015;7(6):779–96.
20. Reschgenger U, Gorris HH. Perspectives and challenges of photon-upconversion nanoparticles–Part I: routes to brighter particles and quantitative spectroscopic studies. Anal Bioanal Chem. 2017;409(25):5855–74.
21. Wang M, Fang L, Li M, Liu Z, Hu Y, Zhang X. Effect of rare earth dopant onthermal stability and structure of $ZnO$-$B_2O_3$-$SiO_2$. J Inorg Mater. 2017;32:643–8.
22. Gorris HH, Resch-Genger U. Perspectives and challenges of photon-upconversion nanoparticles–Part II: bioanalytical applications. Anal Bioanal Chem. 2017;409(7):1–16.
23. Lourenco AV, Kodaira CA, Ramos-Sanchez EM, Felinto MC, Goto H, Gidlund M, et al. Luminescent material based on the Eu(TTA)3(H2O)2 complex incorporated into modified silica particles for biological applications. Inorg Chim Acta. 2013;123(6):11–7.
24. Zhang Y, Tang Y, Liu X, Zhang L, Lv Y. A highly sensitive upconverting phosphors-based off–on probe for the detection of glutathione. Sensors Actuators B. 2013;185(8):363–9.
25. Eliseeva SV, Bunzli JC. Lanthanide luminescence for functional materials and bio-sciences. Chem Soc Rev. 2010;39(1):189–227.
26. Babailov SP. Thulium diketonate as NMR paramagnetic probe for moderately fast molecular dynamics and supersensitive reagent for in situ control of temperature. Sensors Actuators B. 2016;233:476–8.
27. Yang W, Xia J, Zhou G, Jiang D, Li Q, Wang S, et al. Luminescent oxygen-sensing film based on β-diketone-modifiedEu(III)-doped yttrium oxide nanosheets. Sensors Actuators B. 2018;257:340–6.
28. Liu SG, Pan RK, Zhou XP, Wen XL, Chen YZ, Wang S, et al. Blue-light exci europium(III) complex based on deprotonated1-(9-ethyl-6,8-dimethyl-9H-carbazol-2-yl) -4,4,4- trifluorobutane-1,3 -dionate and 1,10-phenanthroline. Inorg Chim Acta. 2013;395(2):119–23.
29. R. W, Su Q. A study of intramolecular energy relaxation processes of rare earth complexes [$Ln(TTA)_3{\cdot}2H_2O$, Ln = Nd, Eu, Gd]. J Mol Struct. 2000;559(1):195–9.
30. Parra DF, Forster PL, Łyszczek R, Ostasz A, Lugao AB, Rzączyńska Z. Thermal behavior of the highly luminescent poly(3-hydroxybutyrate):$Eu(tta)_3(H_2O)_2$ red-emissive complex. J Therm Anal Calorim. 2013;114(3):1049–56.
31. Faustino WM, Nunes LA, Terra IAA, Felinto MCFC, Brito HF, Malta OL. Measurement and model calculation of the temperature dependence of ligand-to-metal energy transfer rates in lanthanide complexes. J Lumin. 2013;137:269–73.
32. Fernandes M, de Zea Bermudez V, Ferreira RAS, Carlos LD, Martins NV. Incorporation of the $Eu(tta)_3(H_2O)_2$ complex into a co-condensed d-U(600)/d-U(900) matrix. J Lumin. 2008;128(2): 205–12.
33. Ellairaja S, Shenbagavalli K, Ponmariappan S, Vasantha VS. A green and facile approach for synthesizing imine to develop optical biosensor for wide range detection of bilirubin in human biofluids. Biosens Bioelectron. 2017;91(17):82–8.
34. Toietta G, Mane VP, Norona WS, Finegold MJ, Ng P, McDonagh AF, et al. Lifelong elimination of hyperbilirubinemia in the Gunn rat with a single injection of helper-dependent adenoviral vector. Proc Natl Acad Sci U S A. 2005;102(11):3930–5.
35. Nie Z, Fung YS. Microchip capillary electrophoresis for frontal analysis of free bilirubin and study of its interaction with human serum albumin. Electrophoresis. 2008;29(9):1924–31.
36. Zelenka J, Lenícek M, Muchová L, Jirsa M, Kudla M, Balaz P, et al. Highly sensitive method for quantitative determination of bilirubin in biological fluids and tissues. J Chromatogr B. 2008;867(1):37–42.

37. Iwatani S, Nakamura H, Kurokawa D, Yamana K, Nishida K, Fukushima S, et al. Fluorescent protein-based detection of unconjugated bilirubin in newborn serum. Sci Rep. 2016;6:28489–97.
38. Luye M, Droujinine IA, Rajan NK, Sawtelle SD, Reed MA. Direct, rapid, and label-free detection of enzyme-substrate interactions in physiological buffers using CMOS-compatible nanoribbon sensors. Nano Lett. 2014;14(9):5315–22.
39. Noh HB, Won MS, Shim YB. Selective nonenzymatic bilirubin detection in blood samples using a Nafion/Mn-Cu sensor. Biosens Bioelectron. 2014;61(1):554–61.
40. Ponhong K, Teshima N, Grudpan K, Vichapong J, Motomizu S, Sakai T. Successive determination of urinary bilirubin and creatinine employing simultaneous injection effective mixing flow analysis. Talanta. 2015;133:71–6.
41. Liu SG, Gong ML, Wang S, Tan XM. A luminescent Eu(III) complex based on 2-(4', 4', 4'-trifluoro-1', 3'-dioxobutyl)-dibenzothiophene for light-emitting diodes. Spectrochim Acta–Part A. 2009;74(3):731–4.
42. Novotna P, Kralik F, Urbanova M. Chiral recognition of bilirubin and biliverdin in liposomes and micelles. Biophys Chem. 2015;205:41–50.
43. Kuenzle CC, Pelloni RR, Weibel MH. A proposed novel structure for the metal chelates of bilirubin. Biochem J. 1972;130(4):1147–50.
44. Zhuang QK, Dai HC, Liu H. Electrochemical study on the interaction of bilirubin with europium ions in aqueous media. Electroanalysis. 2015;11(18)):1368–71.
45. Millan S, Satish L, Kesh S, Chaudhary YS, Sahoo H. Interaction of lysozyme with rhodamine B: a combined analysis of spectroscopic and molecular docking. J Photochem Photobiol B. 2016;162:248–57.
46. Correa RS, Oliveira KM, Pérez H, Plutín AM, Ramos R, Mocelo R, et al. cis-bis(*N*-benzoyl-*N′*,*N′*-dibenzylthioureido)platinum(II): synthesis, molecular structure, and its interaction with human and bovine serum albumin. Arab J Chem. 2015; https://doi.org/10.1016/j.arabjc.2015.10.006.
47. Roy AS, Ghosh P, Dasgupta S. Glycation of human serum albumin affects its binding affinity towards (−)-epigallocatechin gallate. Inclusion phenom. Macrocycl Chem. 2016;85(3/4):193–202.
48. Porter PS, Ward RC, Bell HF. The detection limit. Environ Sci Technol. 1988;22(8):856–61.
49. Murray JS, Lane P, Politzer P. Simultaneous σ-hole and hydrogen bonding by sulfur- and selenium-containing heterocycles. Int J Quantum Chem. 2008;108(15):2770–81.
50. Iwaoka M, Isozumi N. Hypervalent nonbonded interactions of a divalent sulfur atom. Implications in protein architecture and the functions. Molecules. 2012;17(6):7266–83.
51. Lu J, Lu Y, Yang S, Zhu W. Theoretical and crystallographic data investigations of noncovalent S·O interactions. Struct Chem. 2011;22(4):757–63.
52. Shishkin OV, Omelchenko IV, Kalyuzhny AL, Paponov BV. Intramolecular S···O chalcogen bond in thioindirubin. Struct Chem. 2010;21(5):1005–11.
53. Politzer P, Murray JS, Clark T. Halogen bonding and other sigma-hole interactions: a perspective. Phys Chem Chem Phys. 2013;15(27):11178–89.
54. Gangan TVU, Sreenadh S, Reddy MLP. Visible-light exci highly luminescent molecular plastic materials derived from $Eu^{3+}$ -biphenyl based β-diketonate ternary complex and poly(methylmethacrylate). J Photochem Photobiol A. 2016;328:171–81.